DALTON
FULL PAPER

Nitrogen *versus* oxygen co-ordination of carboxamide-functionalized triazacyclononane ligands in transition metal ion complexes

Thomas Weyhermüller, Karl Weighardt and Phalguni Chaudhuri *

Max-Planck-Institut für Strahlenchemie, PO Box 101365, D-45413 Mülheim an der Ruhr, Germany. E-mail: chaudh@mpi-muelheim.mpg.de

Received 17th August 1998, Accepted 22nd September 1998

Mononuclear complexes of zinc(II), copper(II), nickel(II), cobalt(II), iron(II), manganese(II), chromium(III), vanadium(III) and vanadyl(IV) with the ligands 1,4,7-tris(carbamoylmethyl)-1,4,7-triazacyclonanone (L) and its *N*-methyl derivative $C_6H_{12}N_3(CH_2CONHMe)_3$ (MeL) have been prepared and structurally, magnetochemically and spectroscopically characterized. The ligands on complexation provide, in general, the MN_3O_3 moiety, *i.e.* they co-ordinate through the carboxamide oxygens with the exception of chromium(III). Chromium(III) forms complexes not only with the carboxamide oxygens, but also with the deprotonated amide nitrogen, thus yielding both CrN_3O_3 and CrN_4O_2 chromophores, respectively, which have been confirmed by crystal structures. The crystal structure of the VO^{2+} complex reveals a typical six-co-ordinate geometry with one amide dangling free, while that of the vanadium(III) compound shows seven-co-ordinate pentagonal bipyramidal geometry with the amide co-ordinated to the metal *via* its carbonyl oxygen atoms together with a chloride ion. The pendant carboxamide groups hydrolyse slowly to the corresponding carboxylic acid groups. The ligands L and MeL provide weak ligand fields and, relative to the trimethyl substituted cyclic amine [9]aneN_3, *i.e.* 1,4,7-trimethyl-1,4,7-triazacyclononane, are more effective in stabilizing the metal centers in the oxidation state II.

Introduction

This work stems from our interest in utilizing 1,4,7-triazacyclononane (TACN) based ligands for the synthesis of high- and low-valent organometallics as well as for the preparation of models of metalloprotein active sites.[1] Owing to the kinetic and thermodynamic stability which these macrocycles impart upon their complexes, they have become highly valued as supporting ligands not only for the synthesis of monomeric and homopolynuclear but also for heteropolynuclear complexes.[2]

This macrocyclic amine is readily derivatized at the nitrogen atoms,[3–5] resulting in C_3-symmetric *N*,*N*′,*N*″-trisubstituted ligands. A variety of pendant-arm ligands such as CH_2CO_2H,[6,7] CH_2CH_2OH,[8] $CH_2C_6H_4OH$,[9] $CH_2C_6H_4SH$,[10] $CH_2C_6H_4NH_2$,[11] $CH_2CH_2NH_2$,[12] $CH_2C_5H_4N$,[13,14] bipyridylmethyl,[15] imidazolylmethyl,[16] pyrazolylmethyl,[17] $CH_2CONHCH(CH_2Ph)CO_2Me$,[18] $CH_2CH_2C(NH_2)$=NOH[19] and $CH_2C(Me)$=N–OH[19] have been prepared to generate a battery of ligands possessing divergent steric and electronic properties and co-ordination environments. Our interest in this type of functionalization has prompted us to prepare pendant-amide ligands based on TACN.

Ligands with pendant-amide groups, CH_2CONH_2, are particularly interesting because they can form complexes in which the NH_2 group can remain protonated and the metal co-ordination of the CH_2CONH_2 group occurs through the carbonyl oxygen, or the NH_2 group can deprotonate and so act as a deprotonated amide nitrogen thus providing a strong metal binding site. This co-ordination behavior is very similar to that of the CONH group in small peptides.[20] We believe that this study provides new information on the metal–peptide bonding mode,[21] which at present is still scarcely explored. The ligand 1,4,7-tris(carbamoylmethyl)-1,4,7-triazacyclononane (L) has the advantage of yielding complexes containing both carbonyl oxygens and amide nitrogens as donor atoms. Additionally, it might stabilize unusual higher oxidation states of metal centers through its deprotonated N-amidate group. It is also interesting to compare the ligating property of the CH_2CONH^- with that of the $CH_2CO_2^-$ group.[7]

We found that the divalent metal ions are ineffective in promoting amide nitrogen deprotonation, but a trivalent metal ion like Cr^{III} can easily deprotonate the NH_2 group in the ligand. Our goal is to characterize the interaction of the chromium(III) ion with the amide bond and to compare it with that of the other metals with the peptide ligands.

In this paper we describe the mononuclear complexes of Zn^{II}, Cu^{II}, Ni^{II}, Co^{II}, Fe^{II}, Mn^{II}, Cr^{III}, V^{III} and VO^{2+} with the new ligands L and its *N*-methyl derivative MeL and their characterization by spectroscopic methods together with structural characterization of five complexes. While our research was in progress, the synthesis of L and its complexes with Y^{III} and Lu^{III} were reported.[22a] Very recently Berreau *et al.*[22b] have described copper complexes of 1,4-diisopropyl-1,4,7-triazacyclononane linked to secondary and tertiary amide groups and where their results and present work overlap good agreement is observed.

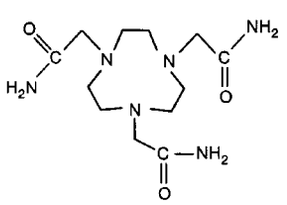

L

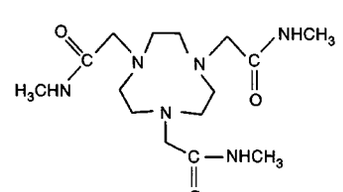

MeL

Experimental

The macrocyclic amine 1,4,7-triazacyclononane was prepared according to a modified method[23] described by Atkins *et al.*[24] All other chemicals were obtained from commercial sources and used as received. Microanalyses were performed by Mikroanalytisches Laboratorium Dornis and Kolbe, Mülheim an der Ruhr. The perchlorate anion was determined gravi-

metrically as tetraphenylarsonium perchlorate. Solution electronic spectra were measured on a Perkin-Elmer Lambda 19 spectrophotometer, Fourier transform infrared spectroscopy on KBr pellets on a Perkin-Elmer 2000 FT-IR instrument. Magnetic susceptibilities of the polycrystalline samples were recorded on a SQUID magnetometer (MPMS, Quantum Design) in the temperature range 2–290 K with an applied field of 1 T. Experimental susceptibility data were corrected for the underlying diamagnetism using Pascal's constants. Mass spectra were recorded either in the ESI or FAB mode using a VG 8200 spectrometer.

Ligand syntheses

1,4,7-Tris(carbamolymethyl)-1,4,7-triazacyclononane L was synthesized by a modification of the reported method.[22] To a solution of 1,4,7-triazacyclononane (5.56 g, 43 mmol) in distilled ethanol (240 ml) was added 2-bromoacetamide (20.0 g, 145 mmol) with stirring at room temperature. The clear solution was charged with either solid sodium methoxide (7.0 g, 130 mmol) or sodium hydroxide (5.20 g, 130 mmol) and the mixture refluxed for 8 h. The precipitated NaBr was filtered off and discarded. The solvent ethanol was evaporated from the filtrate under reduced pressure to yield a white solid (11.6 g), which was recrystallized from ethanol–water (400 : 100 ml). The microcrystalline product, collected in three crops during 48 h, was filtered off, washed with diethyl ether and air-dried. Yield: 9.15 g (≈70%). Mp 233–235 °C (Found: C, 48.2; H, 8.10; N, 28.0. Calc. for $C_4H_8N_2O$: C, 47.99; H, 8.05; N, 27.98%). ^{1}H NMR (D_2O): δ 2.80 (s, 12 H, TACN ring CH_2) and 3.35 (s, 6 H, carboxamide CH_2). IR (KBr, cm^{-1}): 3402s, 3303s (br), 3169s (br), 1711ms and 1655s (br). MS: *m*/*z* 301[M] and 187 (100% abundance).

The *N*-methyl derivative of the ligand, MeL, $C_6H_{12}N_3$-$(CH_2CONHMe)_3$ was prepared by carbamoylalkylation of 1,4,7-triazacyclononane with 2-bromo-*N*-methylacetamide.[25,26] 1,4,7-Triazacyclononane (6.25 g, 48 mmol) was stirred in dry acetonitrile (500 ml) under an atmosphere of argon. Potassium carbonate (20.8 g, 150 mmol) and 2-bromo-*N*-methylacetamide (22.8 g, 150 mmol) were added, and the mixture was heated to reflux for 36 h. The mixture was then cooled to room temperature, the inorganic salts were filtered off and the filtrate was evaporated under reduced pressure. The waxy orange-yellow solid was purified by repeated crystallization from acetonitrile–ether to yield a white solid. Yield: 6.5 g (≈40%) (Found: C, 51.7; H, 8.7; N, 23.9. Calc. for $C_5H_{10}N_2O$: C, 52.61; H, 8.83; N, 24.54%). ^{1}H NMR (CD_3OD): δ 2.77/2.76 (two s, 21 H tacn ring CH_2 + carboxamide CH_3) and 3.25 (s, 6 H, carboxamide CH_2). MS: *m*/*z* 342[M] and 215 (100% abundance). IR (KBr, cm^{-1}): 3323s, 3291s, 1655s and 1565s.

Preparation of complexes

[V(Cl)L][ClO$_4$]$_2$·2MeOH 1. All operations were done under an argon atmosphere. A suspension of the amide ligand L (0.3 g, 1 mmol) and [V(MeCN)$_3$Cl$_3$] (0.28 g, 1 mmol) in methanol (50 ml) was stirred under argon for 1 h, during which time it changed from green to rose. The suspension was filtered to remove the colored solid and the orange-red filtrate treated with a solid sample of $NaClO_4$·H_2O (0.5 g). The solution yielded after 24 h orange crystals, which became turbid on exposure to air. The crystals were preserved under argon to avoid the loss of solvent molecules. Yield: 0.18 g (≈28%) (Found: C, 25.8; H, 4.4; N, 12.9; V, 8.0; ClO_4, 31.9. Calc. for $C_{12}H_{24}Cl_3N_6O_{11}V$·$2CH_3OH$: C, 25.88; H, 4.96; N, 12.93; V, 7.84; ClO_4, 30.61%). IR (KBr, cm^{-1}) 3398s, 3280s, 1661s, 1584s, 1088s and 626m. UV/VIS in water: λ_{max}/nm (ε/M^{-1} cm^{-1}) 363(14.9), 479(24.8), 807(29.8), ≈970 (sh) and ≈1031 (sh) (24.8).

[V(O)L]Br[ClO$_4$]·MeOH 2. A suspension of the ligand L (0.3 g, 1 mmol) and [Et$_4$N]$_2$[VOBr$_4$] (0.65 g, 1 mmol) in methanol (50 ml) was stirred in a closed vessel for 20 h to obtain a blue-green solution. The solution was filtered to remove any solid particles and to the filtrate was added $NaClO_4$·H_2O (0.42 g). The solution yielded after 3 d blue crystals of complex **2**, which were filtered off and air-dried. Yield: 0.38 g (66%) (Found: C, 27.8; H, 4.7; Br, 13.6; N, 14.5; V, 8.6; ClO_4, 18.1. Calc. for $C_{12}H_{24}BrClN_6O_8V$·CH_3OH: C, 26.98; H, 4.88; Br, 13.81; N, 14.52; V, 8.80; ClO_4, 17.19%). IR(KBr, cm^{-1}) 3425s (sharp), 3332s (br), 3220m, 3171m, 1680s, 1663s, 1114s, 978m and 623m. UV/VIS in water: λ/nm (ε/M^{-1} cm^{-1}) 583(40) and 765(25).

[Cr(L − H)]Cl[PF$_6$]·Me$_3$OH 3. To an argon-scrubbed suspension of L (0.60 g, 2 mmol) in methanol (100 ml) was added $CrCl_2$ (0.32 g, 2 mmol) under argon with constant stirring. The stirring was continued for 2.5 h at ambient temperature to obtain an aubergine colored solution with negligible amount of green solid, presumably unchanged $CrCl_2$. The solution was filtered in the air to remove the insoluble particles. To the resulting violet solution was added $NaPF_6$ (0.74 g, 4.4 mmol) and the clear solution, kept in a closed vessel for 24 h, yielded red-violet crystals of complex **3**, which were filtered off and air-dried. Yield: 0.26 g (23%) (Found: C, 27.3; H, 4.7; Cl, 6.1; Cr, 9.0, N, 14.9. Calc. for $C_{12}H_{23}ClCrF_6N_6O_3P$·$CH_3OH$: C, 27.69; H, 4.83; Cl, 6.29; Cr, 9.22; N, 14.91%). IR (KBr, cm^{-1}) 3413s, 3351m, 3256m, 3012m, 1674m, 1609s, 1566s, 841s and 558m. UV/VIS(KBr): 273 (br) and 507 nm. UV/VIS in water: λ_{max}/nm (ε/M^{-1} cm^{-1}) 383(218) and 509(261). μ_{eff}/μ_B (*T*/K): 3.70(290), 3.69(180), 3.64(80), 3.49(10) and 3.28(2).

[Cr(L − H)][ClO$_4$]$_2$ 3*. This microcrystalline perchlorate salt was obtained similarly by using, in place of $NaPF_6$, $NaClO_4$, giving a better yield (66%).

[CrL][ClO$_4$]$_3$ 4. Complex **4** was obtained by adding concentrated $HClO_4$ (1.5 ml) to the violet solution (in the preparation of **3**), instead of $NaPF_6$. Microcrystalline pink-violet **4** was filtered off and air-dried. Yield: 0.45 g (69%) (Found: C, 22.2; H, 3.7; Cr, 7.9; N, 12.8; ClO_4, 43.9. Calc. for $C_{12}H_{24}Cl_3CrN_6O_{15}$: C, 22.15; H, 3.72; Cr, 8.00; N, 12.92; ClO_4, 45.88%). IR (KBr, cm^{-1}) 3368s, 3269m, 3208m, 1677s (sharp), 1567m, 1089s and 625m. UV/VIS in water: λ_{max}/nm (ε/M^{-1} cm^{-1}) 387(150) and 512(256). μ_{eff}/μ_B (*T*/K): 3.70(290), 3.69(210), 3.68(150) and 3.65(100).

[Cr(MeL)][ClO$_4$]$_3$·3.5H$_2$O 5. An argon-scrubbed solution of MeL (0.34 g, 1 mmol) in methanol (50 ml) was treated with 0.16 g (1.3 mmol) of $CrCl_2$ and the suspension stirred under argon for 6 h. The resulting suspension was filtered to remove a green solid, presumably an excess of $CrCl_2$, in the air and to the violet filtrate perchloric acid (1 ml) was added. The precipitated red solid was collected after 1 h by filtration and air-dried. The solid was recrystallized from water acidified with $HClO_4$ (pH ≈ 1) at 60 °C to yield X-ray quality red crystals. Yield: 0.5 g (66%) (Found: C, 23.9; H, 4.9; Cr, 7.0; N, 11.3; ClO_4, 39.1. Calc. for $C_{15}H_{30}Cl_3CrN_6O_{15}$·$3.5H_2O$: C, 23.83; H, 4.93; Cr, 6.88; N, 11.12; ClO_4, 39.47%). IR(KBr, cm^{-1}) 3432s (br), 1659s, 1542m, 1109, 1088s and 626m. UV/VIS in water (pH ≈ 3): λ/nm (ε/M^{-1} cm^{-1}) 389(162) and 513(278). μ_{eff}/μ_B (*T*/K): 3.83(290), 3.82(160), 3.80(15 K), 3.75(5) and 3.59(2).

Compound **5** could also be obtained by recrystallizing **6** from water, acidified with $HClO_4$ (pH ≈ 1).

[Cr(MeL − H)][ClO$_4$]$_2$·MeOH 6. A solution of MeL (0.34 g, 1 mmol) in dry methanol (50 ml) was treated with solid $CrCl_2$ (0.12 g, 1 mmol) under argon. The suspension was stirred under argon for 1 h at ambient temperature and left overnight. The resulting violet solution was filtered to remove any solid particles and the filtrate after addition of $NaClO_4$ (0.36 g) concentrated by passing argon through it. The solution yielded after

cooling at 4 °C deep violet crystals of **6**. Yield: 0.17 g (27%) (Found: C, 30.7; H, 5.3; Cr, 8.8; N, 13.4; ClO_4, 32.7. Calc. for $C_{15}H_{29}Cl_2CrN_6O_{11}\cdot CH_3OH$: C, 30.78; H, 5.33; Cr, 8.33; N, 13.46; ClO_4, 31.86%). IR(KBr, cm^{-1}) 3535m, 3415m (br), 3324m, 1646s, 1596s, 1088s and 624m. μ_{eff}/μ_B (T/K): 3.80(290), 3.79(150), 3.78(100), 3.74 (15 K), 3.72 (10 K) and 3.43(2).

$[M^{II}L][ClO_4]_2$ (M^{II} = Zn 7, Cu 8, Ni 9, Co 10, Fe 11 or Mn 12). As these complexes were prepared in a very similar way a representative method only is described. An argon-scrubbed solution of $M(O_2CMe)_2\cdot xH_2O$ (1 mmol) in methanol (30 ml) was treated with a sample of the amide ligand L (0.30 g, 1 mmol) under vigorous stirring. The mixture was stirred at room temperature until a clear solution was obtained (*ca.* 2 h). Upon addition of $NaClO_4\cdot H_2O$ (0.6 g) crystalline solids were obtained. The microcrystalline product was collected by filtration and air-dried. Yield: 70–80%. Complex **7** [Found (Calc. for $C_{12}H_{24}Cl_2N_6O_{11}Zn$): C, 25.4(25.53); H, 4.3(4.28); N, 14.8(14.88); Zn, 11.7 (11.61); ClO_4, 35.0(35.23)%], colorless; IR(KBr, cm^{-1}) 3430m, 3380m, 3246m (br), 3107m, 1665s, 1611m, 1596m, 1103s, 1087s and 626m. Complex **8** [Found (Calc. for $C_{12}H_{24}Cl_2CuN_6O_{11}$): C, 25.7(25.61); H, 4.3(4.30); Cu, 10.9(11.29); N, 14.9(14.93); ClO_4, 34.9(35.34)%], blue; IR(KBr, cm^{-1}) ≈3400s (br), 3150m, 1663s, 1591m, 1145s, 1110s, 1088s and 627m; UV/VIS in water λ_{max}/nm (ε/M^{-1} cm^{-1}) 764(96.5); μ_{eff}/μ_B (T/K) 1.97(290), 1.93(200), 1.90(130), 1.85(30), 1.83(10), 1.82(7) and 1.60(2). Complex **9** [Found (Calc. for $C_{12}H_{24}Cl_2N_6NiO_{11}$: C, 25.9(25.97); H, 4.4(4.36); N, 15.2(15.14); Ni, 9.7(10.04); ClO_4, 36.0(35.84)%], violet; IR(KBr, cm^{-1}) 3459m, 3386s, 3336m, 3294m (br), 3133m, 3096s, 1676s, 1622m, 1594m, 1146s, 1115s, 1093s and 627m; UV/VIS in water λ/nm (ε/M^{-1} cm^{-1}) 354(19.6), 561(14.7), 802(19.6) and 920(39.3); UV/VIS in MeCN 358(20.7), 561(15.5), 798(20.7) and 920(41.5); μ_{eff}/μ_B (T/K) 3.13(290), 3.10(200), 3.05(30), 3.04(10), 3.00(5) and 2.85(2). Complex **10** [Found (Calc. for $C_{12}H_{24}Cl_2CoN_6O_{11}$: C, 25.7(25.82); H, 4.3(4.33); Co, 10.1(10.56); N, 15.0(15.06); ClO_4, 34.9(35.63)%], rose; IR(KBr, cm^{-1}) 3431s, 3355m, 3300m, 3241m, 1665s, 1595m, 1090s (br) and 625m; UV/VIS in water λ_{max}/nm (ε/M^{-1} cm^{-1}) 500(20), 668(5) and 1146(15); μ_{eff}/μ_B (T/K) 4.91(290), 4.97(200), 5.00(100), 4.91(50), 4.59(7) and 3.67(2). Complex **11** [Found (Calc. for $C_{12}H_{24}Cl_2FeN_6O_{11}$): C, 25.8(25.96); H, 4.2(4.36); Fe, 9.1(10.06); N, 15.0(15.14); ClO_4, 35.6(35.83)%], pale yellow; IR(KBr, cm^{-1}) 3374m, 3323w, 3252m, 3094m (br), 1681m, 1659s, 1608m, 1589m, 1144s, 1116s, 1089s and 628m; μ_{eff}/μ_B (T/K) 4.90(290), 4.80(50), 4.60(15), 4.10(5) and 3.21(2). Complex **12** [Found (Calc. for $C_{12}H_{24}Cl_2MnN_6O_{11}$): C, 25.9(26.04); H, 4.4(4.37); Mn, 9.9(9.91); N, 15.0(15.16); ClO_4, 36.0(35.91)%], colorless; IR(KBr, cm^{-1}) 3462m, 3379m (br), 3361s (br), 1695w, 1655s, 1611m, 1145s, 1120s, 1088s and 627m; μ_{eff}/μ_B (T/K) 5.88(290), 5.87(50), 5.85(30), 5.84(20), 5.80(10 K), 5.76(7) and 4.74(2).

The metal complexes of MeL, $[M^{II}(MeL)][ClO_4]_2$ (M^{II} = Zn **13**, Cu **14**, Ni **15**, Co **16**, Fe **17** or Mn **18**, have been prepared in a very similar way. Complex **13** (Found: C, 29.5; H, 4.9; N, 13.8; ClO_4, 33.1. Calc. for $C_{15}H_{30}Cl_2N_6O_{11}Zn$: C, 29.72; H, 4.99; N, 13.86; ClO_4, 32.81%): IR(KBr, cm^{-1}) 3106m, 1634s, 1145s, 1086s and 625m; ^1H NMR (D_2O) δ 2.74–2.67 (m), 2.81 (s), 2.88–2.95 (m) and 3.66 (s); ^{13}C NMR (D_2O): δ 27.04, 33.40 (CH_3N), 50.56 (CH_2N), 57.90 (CH_2CO) and 173.71 (C=O); ESI-MS (MeCN) m/z 505.1 (40, M − ClO_4) and 405.1 (100%, M − $2ClO_4$). Complex **14** (Found: C, 29.16; H, 5.0; Cu, 9.5; N, 13.6; ClO_4, 33.0. Calc. for $C_{15}H_{30}Cl_2CuN_6O_{11}$: C, 29.79; H, 4.99; Cu, 10.51; N, 13.89; ClO_4, 32.88%): IR(KBr, cm^{-1}) 3364s, 3233m, 3091m, 1638s, 1619s, 1145s, 1115s, 1086s and 626m; UV/VIS in water λ_{max}/nm (ε/M^{-1} cm^{-1}) 767(96.6); μ_{eff}/μ_B (T/K) 1.82(5.0) and 1.94(150.0); ESI-MS (MeCN) m/z 504 (M − ClO_4) and 404.2 (100%, M − $2ClO_4$). Complex **15** (Found: C, 29.2; H, 5.1; N, 13.7; Ni, 9.6; ClO_4, 32.9. Calc.: C, 30.03; H, 5.04; N, 14.01; Ni, 9.78; ClO_4, 33.15%). IR(KBr, cm^{-1}) 3426s, 3233m, 3073m, 1630s, 1145s, 1117s, 1088s and 626m; UV/VIS in water λ_{max}/nm (ε/M^{-1} cm^{-1}) 357(19.3), 561(14.5) and 918(43.5); μ_{eff}/μ_B (T/K) 2.95(7.0) and 3.00(150); ESI-MS (MeCN) m/z 499.2 (50, M − ClO_4) and 399.1 (100%, M − $2ClO_4$). Complex **16** (Found: C, 29.4; H, 4.9; Co, 9.6; N, 13.9; ClO_4, 33.1. Calc.: C, 30.01; H, 5.04; Co, 9.82; N, 14.00; ClO_4, 33.13%): IR(KBr, cm^{-1}) 3430s, 3246s, 3106s, 1630s, 1145s, 1081s and 625m; UV/VIS in water λ_{max}/nm (ε/M^{-1} cm^{-1}) 507(20.4), 659(6.8) and 1160(15.3); μ_{eff}/μ_B (T/K) 2.86(2.0), 3.24(5.0), 3.36(10) and 3.73(150); ESI-MS(MeCN) m/z 500.2 (90, M − ClO_4) and 400.2 (100%, M − $2ClO_4$). Complex **17** (Found: C, 28.9; H, 5.2; Fe, 9.0; N, 13.8; ClO_4, 33.0. Calc.: C, 30.17; H, 5.06; Fe, 9.33; N, 14.07; ClO_4, 33.31%): IR(KBr, cm^{-1}) 3378s, 3277s, 3109m, 1631s, 1148mn, 1090s and 624m; μ_{eff}/μ_B (T/K) 4.01(2.0), 4.79(5.0), 5.09(10) and 5.07(150); ESI-MS(MeCN) m/z 497 (100%, M − ClO_4) and 397.0 (91%, M − $2ClO_4$). Complex **18** (Found: C, 29.4; H, 5.0; Mn, 8.3; N, 13.8; ClO_4, 33.9. Calc.: C, 30.21; H, 5.07; Mn, 9.21; N, 14.09; ClO_4, 33.36%): IR(KBr, cm^{-1}) 3402s, 3245m, 3091m, 1632s, 1144s, 1106s, 1088s and 626m; μ_{eff}/μ_B (T/K) 5.72(5.7), 5.77(10.0), 5.80(20) and 5.81(290); ESI-MS(MeCN) m/z 496.2 (100, M − ClO_4) and 396.2 (43%, M − $2ClO_4$).

$[V(MeL)Cl][ClO_4]_2$ 19. This orange crystalline compound was obtained in the same way as **1** (Found: C, 29.3; H, 4.7; Cl, 5.5; N, 13.5; ClO_4, 32.0. Calc. for $C_{15}H_{30}Cl_3N_6O_{11}V$: C, 28.70; H, 4.82; Cl, 5.64; N, 13.39; ClO_4, 31.69%): IR(KBr, cm^{-1}) 3395s, 3105m, 1639s, 1165m, 1091s and 624m; μ_{eff}/μ_B (T/K) 2.23(2), 2.70(7.1), 2.71(10) and 2.75(150).

Crystallography

The crystallographic data of $[V^{III}(Cl)L][ClO_4]_2\cdot 2MeOH$ **1**, $[V^{IV}(O)L]Br[ClO_4]\cdot MeOH$ **2**, $[Cr^{III}(L-H)]Cl[PF_6]\cdot MeOH$ **3**, $[Cr^{III}(MeL)][ClO_4]_3\cdot 3.5H_2O$ **5** and $[Ni^{II}L][ClO_4]_2$ **9** are summarized in Table 1. Graphite monochromated Mo-Kα X-radiation (λ 0.71073 Å) was used throughout. Intensity data collected at 293 K for complex **9** and 100 K for **1**, **2**, **3** and **5** were corrected for Lorentz-polarization and absorption effects for **1**, **2**, **3** and **5** using the program SADABS.[27] No absorption correction was done for **9**. The structures were solved by direct methods by using SHELXTL-PLUS.[28] The function minimized during full-matrix least-squares refinement was $\Sigma w(|F_o| - |F_c|)^2$. Neutral atom scattering factors and anomalous dispersion corrections for non-hydrogen atoms were taken from ref. 29(*a*). Hydrogen atoms attached to carbon were placed at calculated positions with isotropic thermal parameters. Those bound to nitrogen were located from the difference map. All non-hydrogen atoms were refined with anisotropic thermal parameters. Absolute configurations for **2** and **3** were checked using the Flack X parameter.[29b]

CCDC reference number 186/1172.

See http://www.rsc.org/suppdata/dt/1998/3805/ for crystallographic files in .cif format.

Results and discussion

The ligands L and MeL were prepared using adaptations to the methods described in the literature for their syntheses.[22,26] This involved reaction of 3 equivalents of 2-bromoacetamide or 2-bromo-*N*-methylacetamide with the free amine 1,4,7-triazacyclononane in the presence of a base. The ligands were conveniently isolated in reasonable yields and their purities established by elemental analyses, NMR, IR and mass spectrometry. The transition metal complexes, prepared in methanol from the respective metal salts and the free base form of the ligands L or MeL, were isolated as perchlorate salts.

Although the ligands L and MeL both have potentially dissociable protons present as NH_2 or NHMe groups, respectively, only one of the three groups is deprotonated upon reaction with

chromium(II) chloride. The reaction of $[VOBr_4]^{2-}$ with the ligand L yields blue crystals of $[(V{=}O)L]Br[ClO_4]\cdot MeOH$ **2**, in which the ligand is only pentadentate, the sixth co-ordination site being occupied by a terminal oxo ligand. One carboxamide group is not co-ordinated to the vanadium(IV) center, consistent with the presence of two strong bands in the carbonyl region and a V=O structural unit ($\nu_{V=O} \approx 978$ cm^{-1}). In all other cases the physical data suggest that the ligand is hexadentate, at least, in the solid state.

As the properties of the complexes **13**–**19** containing the methylated ligand MeL are very similar to those of the parent ligand L, and they were characterized similarly, we will refrain mostly from the discussion of the complexes with the ligand MeL.

Characterization

The IR spectra of all the complexes derived from L exhibit characteristic bands due to the ligand [ν(NH), and ν(C=O) at about ≈3200 and ≈1670 cm^{-1}], and non-co-ordinated perchlorate anions (≈1090 and ≈625 cm^{-1}). In the case of **3**, $[Cr(L - H)]^{2+}$, a sharp strong band observed at 1609 cm^{-1} (together with a medium strong band at 1674 cm^{-1}) can be attributed to the presence of the deprotonated amide moiety, while for **4**, $[CrL]^{3+}$, this band is absent and a strong band is observed at 1677 cm^{-1}, a region where the ν(C=O) vibrations for all other compounds appear (see Experimental section). This is a strong indication that in **4**, together with the other compounds, all three carboxamide oxygen atoms are co-ordinated to the metal centers, but not in **3**. This structural proposal has been confirmed by the X-ray structural determinations.

The electronic spectra of divalent and trivalent first-row transition-metal complexes (given in the Experimental section) are consistent with these metal ions being in a pseudo-octahedral environment (facial N_3O_3 donor set). Judged on the basis of absorption coefficients, the bands and the shoulders for **1**, a seven-co-ordinated d^2 species, are ascribed to the d–d transitions of the vanadium(III) centre. In contrast complex **2**, a d^1 VO^{2+} species, displays only two low-intensity d–d transitions at 583 (40) and 765 nm (25 M^{-1} cm^{-1}). These bands are assigned[30] as $^2B_2(d_{xy}) \longrightarrow {}^2B_1(d_{x^2-y^2})$ and $^2B_2(d_{xy}) \longrightarrow {}^2E(d_{xz}, d_{yz})$ transitions, respectively, assuming a C_{4v} symmetry for **2**. This leads to the 10*Dq* value of 17 150 cm^{-1}, which is slightly smaller than that of the corresponding tris(acetate) analog, [VO(TCTA)][7] (TCTA = 1,4,7-triazacyclononane-1,4,7-triacetate) (17 450 cm^{-1}) and in good agreement with the other reported spectra for VO^{2+} species.[31] In the visible region a single absorption band at 764 nm with $\varepsilon = 96.5$ M^{-1} cm^{-1} is observed for the copper(II) complex, **8**; this is similar to the spectrum for the corresponding complex with the ligand containing three acetate groups[7] as pendant arms to the parent macrocycle [9]aneN$_3$, and taken as further evidence that, with the exception of $[VO(L)]^{2+}$ **2**, the ligand L is invariably hexadentate and the copper(II) ion is six-co-ordinate. The visible spectrum of nickel(II) complex **9** has features typical of octahedral nickel(II) complexes with $^3A_{2g} \longrightarrow {}^3T_{2g}$ and $^3A_{2g} \longrightarrow {}^3T_{1g}(F)$ transitions occurring at 920 and 561 nm, respectively. A third band at 354 nm is most likely due to a $^3A_{2g} \longrightarrow {}^3T_{1g}(P)$ transition. The spike of 802 nm is considered to arise from the "spin-flip" transition $^3A_{2g}(^3F) \longrightarrow {}^1E_g(^1D)$. Three spin-allowed transitions, as is expected for the octahedral d^7 complexes, are observed for **10** with a very weak ($\varepsilon = 5$ M^{-1} cm^{-1}) band at 668 nm, which can be attributed to the so-called "two-electron jump" $^4T_{1g} \longrightarrow {}^4A_{2g}$ transition.[31]

Owing to the low symmetry of the $Cr^{III}N_3O_3$ and $Cr^{III}N_4O_2$ moieties the molar absorption coefficients of the d–d transitions in the visible region are large for complexes **3** and **4**. The bands at 509 (261), 383 nm (218 M^{-1} cm^{-1}) for **3** and 512 (256), 387 nm (150 M^{-1} cm^{-1}) for **4** are assigned to the first and second spin-allowed transitions $^4A_{2g} \longrightarrow {}^4T_{2g}$ and $^4A_{2g} \longrightarrow {}^4T_{1g}(F)$, respectively, of the d^3 chromium(III) center, noting that the band assignments have been performed by assuming an octahedral ligand field. It allows us to estimate the splitting parameter 10*Dq* for **3** and **4** to be 19 646 and 19 531 cm^{-1}, respectively, indicating that the ligand-field strengths of L and is deprotonated form L − H (*i.e.* the amide form) are not very different. That **3** with the CrN_4O_2 chromophore is stable in neutral aqueous solution and does not become protonated to form **4** with the CrN_3O_3 chromophore has been shown by the fact that the solid state and solution spectra of **3** are identical. It is also interesting in this connection that the *N*-methyl derivative, MeL, is also of similar ligand-field strength.

Stepwise hydrolysis of the pendant carboxamide groups to the carboxylic groups

That the co-ordinated carboxamide ligands are amenable to hydrolysis, resulting in carboxylic acids, is evidenced from the isolation of three chromium(III) complexes containing one, two or three co-ordinated pendant carboxylate groups, respectively; the reaction conditions are shown in Scheme 1.

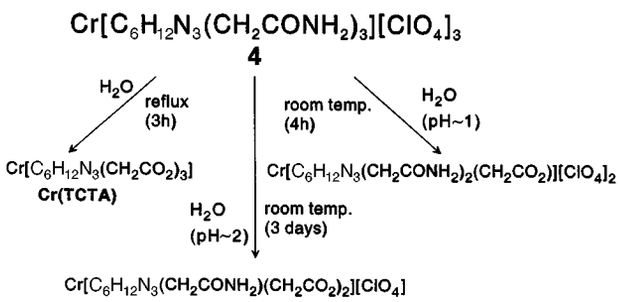

Scheme 1

An aqueous solution of **4**, $[CrL][ClO_4]_3$, on refluxing yielded red needles of the reported [Cr(TCTA)].[7] On the other hand, an aqueous solution of **4**, adjusted to pH ≈1 by addition of perchloric acid and stirred at room temperature for 4 h, afforded upon evaporation of water red crystals of the chromium compound containing two pendant $CONH_2$ ligands and one CO_2^- group. When the above solution is stirred for 3 d the chromium compound containing only one pendant carboxamide and two acetate groups is obtained. Interestingly, the absorption maxima for the d–d bands of the above mentioned four compounds do not vary at all, *viz*. 512 and 387 nm. We will describe in detail the reactions of the above compounds in a future publication.

Similarly compound **11**, the iron(II) complex, in water yields on refluxing in the presence of air the expected hydrolysed product $[Fe^{III}(TCTA)]$.[7]

Crystal structures

The seven-co-ordinate structure for the cation $[V^{III}(Cl)L]^{2+}$ is shown in Fig. 1. Among the co-ordination polyhedra[33] considered as being ideal for this co-ordination number are the 1:5:1 pentagonal bipyramid (D_{5h}), the 1:4:2 monocapped trigonal prism (C_{2v}), the 1:3:3 monocapped octahedron (C_{3v}) and the 4:3 tetragonal base-trigonal cap piano stool (C_s) structures. An analysis of the metal geometry showed that the structure of the cation in **1** could not clearly be assigned to any of these polyhedral forms. However, the geometry approximates with moderate distortions that of the 1:5:1 pentagonal bipyramid. The axial angle Cl(3)–V(1)–N(2) of 169.6° differs from the ideal 180°, while the angle sum in the approximate plane comprising N(1)N(3)O(3)O(2)O(1) atoms about V(1) is 368.4°. The sum of in-plane angles exceeds 360° by *ca.* 8°, which causes slight ruffling in the positions of the "in-plane" O and N donors, O(2) exhibiting the largest deviation from the mean plane. The deviation from ideal angles of 72.0° presumably occurs to accom-

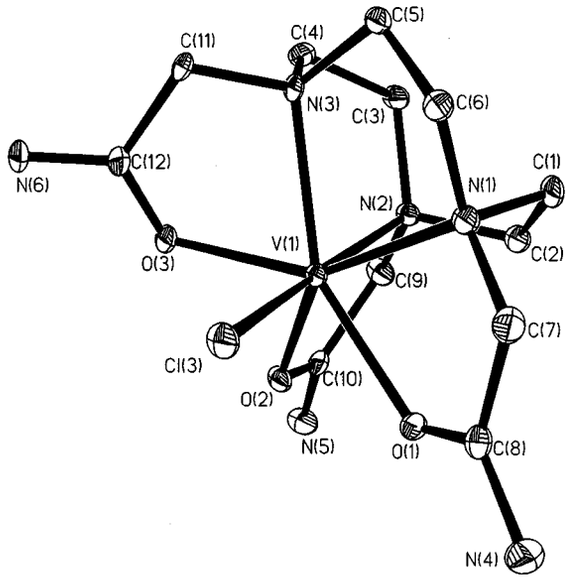

Fig. 1 An ORTEP[32] diagram of the dication $[V^{III}(Cl)L]^{2+}$ in complex **1**.

modate the formation of the five-membered chelate rings of the [9]aneN$_3$ fragment. The largest "in-plane" angle of 79.3°, O(1)–V(1)–O(2), occurs between the co-ordinated oxygens provided by the two neighboring amide pendant arms. Deviation from linearity of the axial ligands is observed even for the six-co-ordinate complexes; for example the axial O–M–N angles in comparable M^{III}(TCTA) complexes[7] are *ca.* 170°.

It has been pointed out[34] that the d^2 electron configuration is well suited to the pentagonal bipyramidal geometry as two electrons are placed in the doubly degenerate d_{xz},d_{yz} orbitals, and thus the d_{xy} and $d_{x^2-y^2}$ are effectively antibonding. The other geometries, having lower symmetry, will not have degenerate orbitals and one electron will have to be placed above the other, thus lowering the maximum possible ligand field stabilization energy and resulting in an orbital singlet ground state.

Selected bond lengths and angles for complex **1** are listed in Tables 2 and 3. The axial V(1)–N(2) distance, 2.088(2) Å, is appreciably shorter than the "in-plane" V(1)–N(3) and V(1)–N(1) distances, 2.213(2) and 2.313(2) Å, respectively. The latter V–N bond distances are comparable to those of related vanadium(III) complexes with aminopolycarboxylate ligands, *e.g.* EDTA.[35] The V–O bond lengths of the donor oxygens O(1), O(2) and O(3) range from 2.095(2) to 2.157(2) Å, which are slightly longer than the comparable V–O distances. The amide nitrogens N(4), N(5) and N(6) exhibit hydrogen bonding with the oxygens O(13) and O(40) of the solvent of crystallization, methanol: N(4)···O(13) 3.180, N(6)···O(13) 2.889 and N(5)···O(40) 2.785 Å.

Blue crystals of complex **2** consist of the dication $[V(O)L]^{2+}$, one non-co-ordinated bromide and perchlorate anion and a methanol molecule of crystallization. Fig. 2 shows the cation together with the atom-labeling scheme; Tables 2 and 3 summarize important bond distances and angles. The vanadium(IV) ion is in a distorted octahedral environment with three tertiary amine nitrogen atoms, two carbamoyl oxygen atoms, and one terminal oxo ligand (*fac*-N_3O_3 donor set). The ligand is only pentadentate; one amide pendant group is not co-ordinated to the vanadium center. The V–O(4) distance is short, 1.606(2) Å, indicating the considerable double-bond character typical of vanadyl(IV) complexes.[36] The V–N(1) bond *trans* to the V=O(4) group is long 2.283(3) Å, which is characteristic for the strong *trans* influence of the V=O group. The other two V–N bonds are shorter, 2.179(2) and 2.114(2) Å. The conformation of the three five-membered V–N–C–C–N chelate rings is (λλλ) or (δδδ). Interestingly, the two five-membered chelate rings built by the

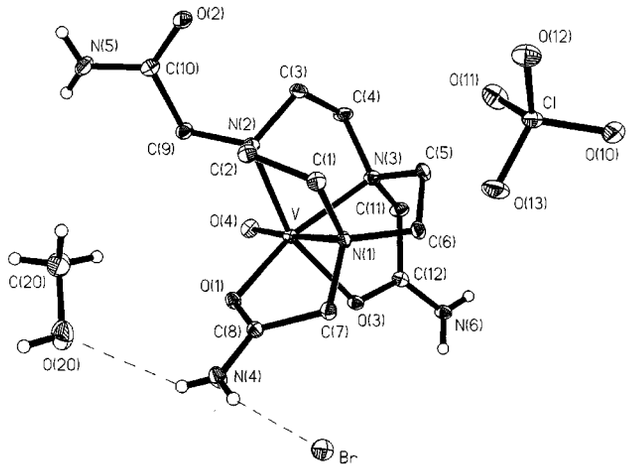

Fig. 2 Molecular structure of $[V(O)L]Br[ClO_4]\cdot MeOH$ **2**.

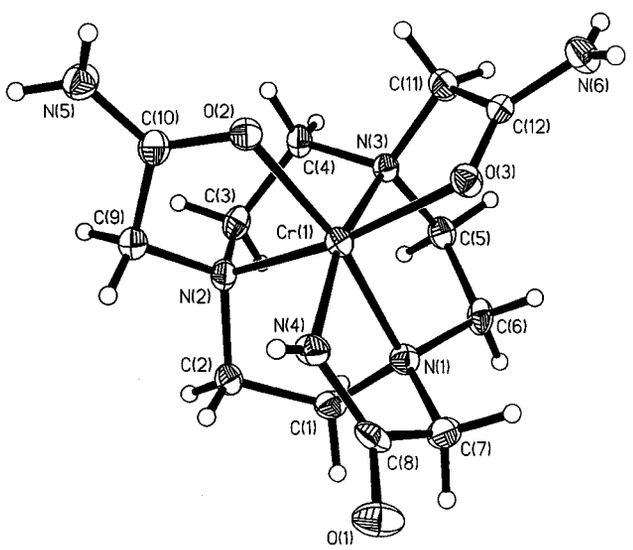

Fig. 3 Structure of the dication $[Cr(L-H)]^{2+}$ in crystals of complex **3**.

co-ordinated carbamoylmethyl groups V–O–C–C–N adopt the (λλ) conformation if the parent cyclononane rings are (δδδ)-configured and *vice versa*.

The molecular structure of the cation in complex **3** is shown in Fig. 3. The geometry about the Cr^{III} is pseudo-octahedral, with three facial sites occupied by the nitrogen donors of the parent cyclononane base fragment, two carbamoyl oxygen atoms, and one deprotonated amide nitrogen of the ligand thus affording a CrN_4O_2 chromophore and completing the co-ordination sphere. Facial co-ordination of the [9]aneN$_3$ moiety results in similar bond angles and distances (Tables 2 and 3), within this portion of the ligand, to those found in other chromium(III) complexes of triazacyclononane derivatives with different pendant arms. Thus, the Cr–N (TACN) distances, 2.054(4), 2.065(4) and 2.068(4) Å, and N–Cr–N bite angles (average 85.9°) to the TACN nitrogens match with those in the [Cr(TCTA)] complex.[7] In contrast to [Cr(TCTA)], a twist angle θ of 47.2° (60° for octahedral co-ordination) indicates a considerable trigonal twisting of the co-ordination environment generated by the N_4O_2 ligand donors. The Cr–O (carbamoyl) bond lengths, 1.987(3) and 1.970(3) Å, are comparable to those reported[37,38] and slightly longer than those in **5**. The conformation of the five-membered chelate rings is very similar to that found in **2**.

The bond length of the deprotonated amide nitrogen to the chromium, Cr–N(4) 1.963(4) Å, is significantly shorter than the Cr–N (amine) bonds, average 2.062(8) Å, reflecting the differ-

Table 1 Crystallographic data for $[V(Cl)L][ClO_4]_2 \cdot 2MeOH$ **1**, $[V(O)L]Br[ClO_4] \cdot MeOH$ **2**, $[Cr(L - H)Cl[PF_6] \cdot MeOH$ **3**, $[Cr(MeL)[ClO_4]_3 \cdot 3.5H_2O$ **5** and $[NiL][ClO_4]_2$ **9**

	1	**2**	**3**	**5**	**9**
Formula	$C_{14}H_{32}Cl_3N_6O_{13}V$	$C_{13}H_{28}BrClN_6O_9V$	$C_{13}H_{27}ClCrF_6N_6O_4P$	$C_{15}H_{37}Cl_3CrN_6O_{18.5}$	$C_{12}H_{24}Cl_2N_6NiO_{11}$
M	649.75	578.71	563.83	755.86	557.98
Crystal size/mm	0.35 × 0.42 × 0.32	0.53 × 0.39 × 0.07	0.18 × 0.25 × 0.21	0.54 × 0.54 × 0.25	1.12 × 0.42 × 0.35
Crystal system	Orthorhombic	Orthorhombic	Orthorhombic	Monoclinic	Monoclinic
Space group	*Pbcn*	$P2_12_12_1$	$P2_12_12_1$	*C*2/*c*	$P2_1/c$
a/Å	13.284(3)	9.877(2)	11.886(1)	29.058(5)	18.034(1)
b/Å	11.925(3)	12.315(3)	16.362(2)	13.680(3)	11.874(1)
c/Å	32.508(6)	17.779(3)	11.335(1)	15.286(3)	10.573(2)
β/°				94.39(3)	106.43(1)
V/Å^3	5150(2)	2162.6(8)	2204.4(4)	6059(2)	2171.6(5)
Z	8	4	4	8	4
D_c/g cm^{-3}	1.676	1.777	1.699	1.657	1.707
Diffractometer	Siemens SMART	Siemens SMART	Siemens SMART	Siemens SMART	Enraf Nonius CAD4
μ/mm^{-1}	0.770	2.489	0.797	0.730	1.207
F(000)	2688	1180	1156	3136	1152
θ_{max}/°	28	33	25	28	26
No. independent reflections [$F > 4.0\sigma(F)$]	5726	8060	3684	6168	4306
Data/parameters	5261/356	6653/300	2975/306	4615/439	2799/301
R_F [$I > 2\sigma(I)$]	0.053	0.036	0.044	0.074	0.066
T/K	100(2)	100(2)	100(2)	100(2)	293(2)

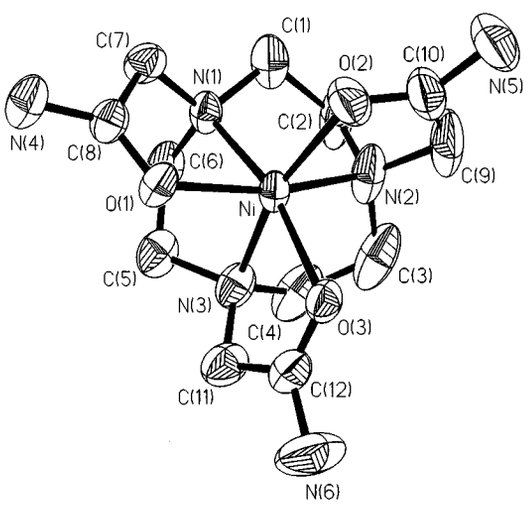

Fig. 4 An ORTEP representation of the $[NiL]^{2+}$ cation of complex **9**.

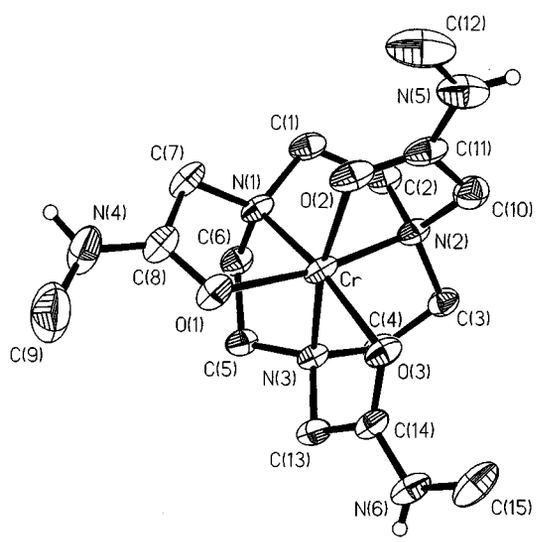

Fig. 5 Perspective view of the trication $[Cr(MeL)]^{3+}$ in complex **5**.

ence between sp^2 and sp^3 hybridization. A very similar relative order of metal–ligand bond lengths[39] M–N (amine) ⩾ M–O (carboxy) > M–N (peptide) is found in the peptide complexes of Co^{III}, Ni^{II}, Cu^{II} and Cr^{III}. It is noteworthy that the Cr–N(3) (amine) bond length *trans* to Cr–N(4) (amide) is not significantly different from those of the other Cr–N (amine) lengths, indicating the absence of the *trans* influence. The hydrogen atom bonded to N(4) was directly located in the Fourier-difference map. The difference between the carbonyl C–O bond lengths for both co-ordinated [O(3)–C(12) 1.271(5) and O(2)–C(10) 1.277(6) Å] and unco-ordinated [O(1)–C(8) 1.254(6) Å] amide carbonyls is small, but not negligible. This is in complete accord with the description that, after deprotonation of the NH_2 group in the amide ligand, the bonding situation between C(8) and O(1) atoms is comparable with that in a ketone >C=O. In other words the delocalization of the π electrons over the whole amide $>C(O)NH_2$ group decreases on deprotonation, rendering a more single bond character to the C–N bond in the pendant arm. The corresponding C–N bond lengths belonging to the pendant arms are as follows: C(12)–N(6) 1.298(7), C(10)–N(5) 1.301(6) and C(8)–N(4) 1.320(6) Å.

The molecular structure of the cation $[NiL]^{2+}$ in complex **9**, as illustrated in Fig. 4, shows that the geometry about the Ni^{II} is pseudo-octahedral, with three facial sites occupied by the nitrogen donors of the macrocycle and three carbonyl oxygens of the pendant amide groups completing the co-ordination sphere. Facial co-ordination of the 1,4,7-triazacyclononane moiety results in similar bond angles and distances, within this portion of the ligand, to those found in other nickel(II) complexes of TACN derivatives with different pendant arms.[40] Thus, the Ni–N distances, 2.070(5), 2.049(5) and 2.051(6) Å, and the N–Ni–N bite angles (average 86.2°) to the TACN nitrogens match those in $[Ni(TCTA)]^-$.[41] The base fragment [9]aneN_3 is chiral once co-ordinated to a metal ion, having (λλλ) or (δδδ) conformation of the five-membered chelate rings M–N–C–C–N. For a given arrangement, the pendant amide groups may attach themselves in a clockwise (Type I) or anticlockwise (Type II) fashion. Type II has been found in **9** similar to $[Ni^{II}(TCTA)]^-$ containing the acetate pendant groups. Considerable trigonal twisting of the amide oxygens relative to the nitrogens of [9]aneN_3 is found in **9** indicating significant distortion from octahedral geometry. The oxygens are rotated by 15.9° ($\theta = 44.1°$) from the expected 60° for octahedral co-ordination.

Fig. 5 shows a perspective view of complex **5**. The structure consists of monomeric, tricationic ions $[Cr(MeL)]^{3+}$. The chromium is co-ordinated to six donor atoms, three nitrogens of the base fragment [9]aneN_3 and three oxygens of

Table 2 Selected bond distances (Å) for complexes **1**, **2**, **3**, **5** and **9**

	1	**2**	**3**	**5**	**9**
M–N(1)	2.313(2)	2.283(2)	2.054(4)	2.041(4)	2.070(5)
M–N(2)	2.088(2)	2.179(2)	2.065(4)	2.039(4)	2.051(6)
M–N(3)	2.213(2)	2.114(2)	2.068(4)	2.046(4)	2.049(5)
M–O(1)	2.157(2)	2.011(2)	—	1.959(4)	2.046(4)
M–O(2)	2.104(2)	—	1.970(3)	1.946(3)	2.026(5)
M–O(3)	2.095(2)	2.019(2)	1.987(3)	1.959(3)	2.073(4)
V–Cl(3)	2.372(1)	—	—	—	—
V=O(4)	—	1.606(2)	—	—	—
Cr–N(4)	—	—	1.963(4)	—	—

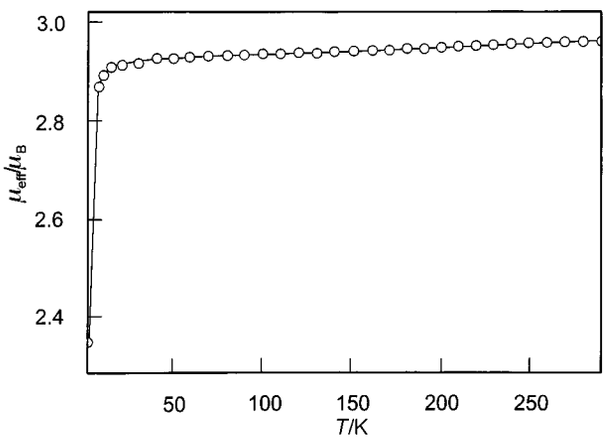

Fig. 6 Plot of μ_{eff} *vs.* T for complex **1**. The solid line is the simulation using the Hamiltonian described in the text.

the amide groups occupying facial positions, respectively of a distorted octahedron. The degree of distortion from the regular octahedral arrangement of the N_3O_3 donor set, expressed by the twist angle θ, is 49°, indicating the propensity of Cr^{III} with d^3 electron configuration for an octahedral environment. The average Cr–N and Cr–O distances, 2.04 and 1.95 Å, respectively are nearly identical to those of [Cr(TCTA)].[7] Bond distances and angles within the [9]aneN_3 fragment in the methyl derivative of the amide ligand are very similar to those observed in **9**, indicating its rigid nature, and selective metrical parameters are summarized in Tables 2 and 3.

Magnetic susceptibility measurements, EPR and Mössbauer spectra

Variable-temperature (2–290 K) magnetic susceptibility data were collected for the vanadium(III) complex **1**. The magnetic moment of 2.32μ_B at 2 K increases monotonically with increasing temperature reaching a value of 2.92μ_B at 290 K; selected values of μ_{eff} are 2.83 μ_B at 7 K, 2.88 μ_B at 30 K, 2.90 μ_B at 100 K and 2.91 μ_B at 200 K. The experimental magnetic data were simulated by a least-squares fitting computer program with a full-matrix diagonalization approach. The Hamiltonian used to describe the paramagnetism is given by eqn. (1) where spin S is

$$H = g\beta HS + D[S_z^2 - \tfrac{1}{3}S(S+1)] \quad (1)$$

1 and D is the axial zero-field splitting parameter. The measured magnetic moments μ_{eff} are reported in Fig. 6, along with the best fit using the above equation. The best fit parameters are $\langle g \rangle = 1.97$ and $D = 3.63$ cm^{-1}. This best fit also required the addition of a temperature-independent paramagnetism term (TIP) of 1.45×10^{-4} cm^3 mol^{-1}. Plots of μ_{eff} *vs.* T with each sign of D showed that very much larger values of D (<−20 cm^{-1}) are required if D is negative. Moreover, all previous values of D for the vanadium(III) ion have been shown to be positive.[42] The g and D values for **1** are in accord with the literature values for vanadium(III) complexes.[43] The deviation from the Curie law for **1** is less pronounced than anticipated, due to partial quenching of the orbital momentum resulting from the covalence ($\kappa < 1$) and the lowering of symmetry, resulting in an orbital singlet ground state. As a result D is positive. Calculations on trivalent vanadium have appeared[44] which lend credence to the presence of a TIP term.

The magnetic moment of 1.69 μ_B at 2 K for complex **2** increases slowly, but steadily, with increasing temperature reaching a value of 1.75 μ_B at 290 K; a few selected μ_{eff} values are 1.70 (5), 1.71 (30), 1.72 (110), 1.73 (170) and 1.74 μ_B (230 K). Several room temperature magnetic susceptibility measurements have been made for both powdered samples and aqueous solutions of vanadyl complexes.[45] The moments all are approximately equal to the spin only value of 1.73 μ_B for one unpaired spin, as is expected when the orbital contribution is completely quenched in the low symmetry field. The experimental magnetic moments were fitted by the theoretical equation containing only the Zeeman term and the temperature-independent contributions to the susceptibility (TIP, so-called high-frequency terms), and the best fit parameters

Table 3 Selected bond angles (°) of complexes **1**, **2**, **3**, **5** and **9**

1			
N(2)–V(1)–O(3)	94.78(9)	N(2)–V(1)–O(2)	77.28(8)
O(3)–V(1)–O(2)	67.76(7)	N(2)–V(1)–O(1)	102.39(8)
O(3)–V(1)–O(1)	138.29(7)	O(2)–V(1)–O(1)	79.30(8)
N(2)–V(1)–N(3)	74.58(8)	O(3)–V(1)–N(3)	72.55(8)
O(2)–V(1)–N(3)	128.43(8)	O(1)–V(1)–N(3)	148.65(8)
N(2)–V(1)–N(1)	90.38(8)	O(3)–V(1)–N(1)	148.06(8)
O(2)–V(1)–N(1)	143.78(8)	O(1)–V(1)–N(1)	70.21(8)
N(3)–V(1)–N(1)	78.57(8)	N(2)–V(1)–Cl(3)	169.61(7)
O(3)–V(1)–Cl(3)	93.54(6)	O(2)–V(1)–Cl(3)	111.74(6)
O(1)–V(1)–Cl(3)	75.15(6)	N(3)–V(1)–Cl(3)	102.11(6)
N(1)–V(1)–Cl(3)	79.28(6)		
2			
O(4)–V–O(1)	101.88(7)	O(4)–V–O(3)	102.02(7)
O(1)–V–O(3)	94.94(6)	O(4)–V–N(3)	104.33(8)
O(1)–V–N(3)	153.77(7)	O(3)–V–N(3)	78.98(7)
O(4)–V–N(2)	93.85(8)	O(1)–V–N(2)	96.49(7)
O(3)–V–N(2)	158.08(7)	N(3)–V–N(2)	82.53(7)
O(4)–V–N(1)	172.67(8)	O(1)–V–N(1)	76.29(6)
O(3)–V–N(1)	85.25(6)	N(3)–V–N(1)	77.78(7)
N(2)–V–N(1)	79.39(7)		
3			
N(4)–Cr(1)–O(2)	98.4(2)	N(4)–Cr(1)–O(3)	79.1(2)
O(2)–Cr(1)–O(3)	94.86(13)	N(4)–Cr(1)–N(1)	81.2(2)
O(2)–Cr(1)–N(1)	167.54(14)	O(3)–Cr(1)–N(1)	97.55(14)
N(4)–Cl(1)–N(2)	97.1(2)	O(2)–Cr(1)–N(2)	82.56(14)
O(3)–Cr(1)–N(2)	165.82(14)	N(1)–Cr(1)–N(2)	85.1(2)
N(4)–Cr(1)–N(3)	165.9(2)	O(2)–Cr(1)–N(3)	95.73(14)
O(3)–Cr(1)–N(3)	82.00(14)	N(1)–Cr(1)–N(3)	85.0(2)
N(2)–Cr(1)–N(3)	84.4(2)		
5			
O(2)–Cr–O(1)	96.7(2)	O(2)–Cr–O(3)	95.27(14)
O(1)–Cr–O(3)	96.41(14)	O(2)–Cr–N(2)	82.4(2)
O(1)–Cr–N(2)	168.74(14)	O(3)–Cr–N(2)	94.85(14)
O(2)–Cr–N(1)	96.8(2)	O(1)–Cr–N(1)	83.13(14)
O(3)–Cr–N(1)	167.90(14)	N(2)–Cr–N(1)	85.8(2)
O(2)–Cr–N(3)	168.3(2)	O(1)–Cr–N(3)	94.9(2)
O(3)–Cr–N(3)	82.49(14)	N(2)–Cr–N(3)	86.4(2)
N(1)–Cr–N(3)	85.5(2)		
9			
O(2)–Ni–O(1)	96.1(2)	O(2)–Ni–N(3)	165.3(2)
O(1)–Ni–N(3)	96.9(2)	O(2)–Ni–N(2)	82.9(3)
O(1)–Ni–N(2)	167.0(2)	N(3)–Ni–N(2)	86.0(3)
O(2)–Ni–N(1)	102.1(2)	O(1)–Ni–N(1)	81.5(2)
N(3)–Ni–N(1)	86.6(2)	N(2)–Ni–N(1)	86.0(2)
O(2)–Ni–O(3)	91.0(2)	O(1)–Ni–O(3)	91.9(2)
N(3)–Ni–O(3)	81.7(2)	N(2)–Ni–O(3)	101.1(2)
N(1)–Ni–O(3)	165.8(2)		

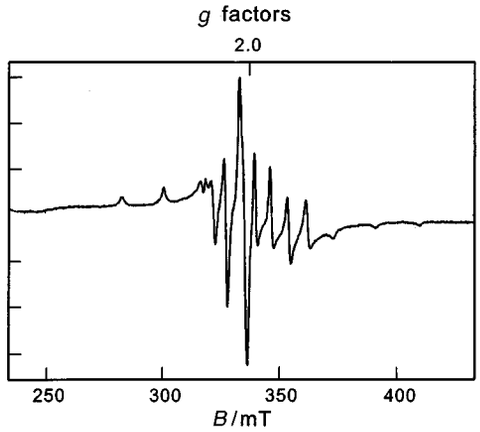

Fig. 7 The X-band EPR spectrum of complex **2** in MeCN at 25 K (microwave frequency 9.450 GHz; power 2.0 mW, modulation amplitude 9.9 G, modulation frequency 100 kHz).

evaluated are $\langle g \rangle = 1.97$ and TIP = 5.04×10^{-4} cm^3 mol^{-1}. This is in good agreement with the g values reported for VO^{2+} ions by EPR measurements.[46] A plot of χ_M *vs.* $1/T$ gives a straight line with slope 0.381 cm^3 mol^{-1} and intercept 238×10^{-6} cm^3 mol^{-1} K^{-1}, which is in good agreement with the theoretical equation for VO^{2+} complexes. Thus magnetic data for **2** indicate an orbitally non-degenerate ground state, and hence the E orbitals are less stable than B_2 in **2**, as is assumed for the band assignment in electronic spectroscopy.

The X-band EPR spectrum of complex **2** in MeCN at 25 K, shown in Fig. 7, demonstrates the low-symmetry structure in the molecule and is very similar to those of other vanadyl complexes reported.[46] The Hamiltonian parameters obtained from the simulation of the spectrum are $g_x = 1.997$, $g_y = 1.995$, $A_x = 65 \times 10^{-4}$ $A_y = 58 \times 10^{-4}$, and $A_z = 165 \times 10^{-4}$ cm^{-1}.

The magnetic moments for complexes **3** (Cr^{III}), **5** (Cr^{III}), **8** (Cu^{II}), **9** (Ni^{II}), **10** (Co^{II}), **11** (Fe^{II}) and **12** (Mn^{II}) have been measured (Experimental section) and are in accord with their high-spin nature. The measured magnetic moments were fitted by the Hamiltonian described above and the best fit parameters are as follows: $\langle g \rangle = 1.89$, $|D| = 1.89$ cm^{-1} for **3**; $\langle g \rangle = 1.97$, $|D| = 0.28$ cm^{-1} for **5**; $\langle g \rangle = 2.10$ for **8**; $\langle g \rangle = 2.145$, TIP = 269×10^{-6} cm^3 mol^{-1} for **9**; $\langle g \rangle = 1.95$, $|D| = 5.8$ cm^{-1}, TIP = 596×10^{-6} cm^3 mol^{-1} for **11**; $\langle g \rangle = 1.98$ for **12**.

The zero-field Mössbauer spectrum of solid complex **11** at 80 K is a symmetrical doublet and yields isomer shift $\delta = 1.09$ mm s^{-1} and quadrupole splitting $\Delta E_Q = 3.98$ mm s^{-1} with linewidths $\Gamma = 0.25$ mm s^{-1}. The Mössbauer isomer shift together with the quadrupole splitting support the six-co-ordinated iron(II) high-spin state for the iron site in **11**.

Conclusion

The hexadentate ligand 1,4,7-tris(carbamoylmethyl)-1,4,7-triazacyclononane and its *N*-methyl derivative form stable complexes with many first-row transition metals in the oxidation states II and III. The co-ordination number is dependent on the metal center, varying between 6 and 7. Octahedral geometry is favored over the prismatic geometry for the ligand of chromium(III) and nickel(II) complexes with twist angles θ of 49 and 44°, consistent with the simple ligand field energy arguments. It is interesting that chromium(III) forms complexes not only with carboxamide oxygens but also with the deprotonated amide nitrogen. Another important point that we note is that vanadium in its oxidation states III and IV forms very stable complexes through the oxygen atoms of the ligand. The d–d transitions of the chromium complex with this ligand are found to be at the same energies as those of the corresponding TCTA complex. The ligand provides a weak ligand field and stabilizes, in general, the +2 oxidation state.

Acknowledgements

We acknowledge the support of this work by the Fonds der Chemischen Industrie. Our thanks are also due to the skillful technical assistance of Frau D. Kreft, Frau H. Schucht and Herr A. Göbels. We also thank Dr. E. Bill for measuring the EPR spectrum.

References

1 P. Chaudhuri and K. Wieghardt, *Prog. Inorg.Chem.*, 1987, **35**, 329.
2 See, for example, D. Burdinski, F. Birkelbach, T. Weyhermüller, U. Flörke, H.-J. Haupt, M. Lengen, A. X. Trautwein, E. Bill, K. Wieghardt and P. Chaudhuri, *Inorg. Chem.*, 1998, **37**, 1009; F. Birkelbach, U. Flörke, H.-J. Haupt, C. Butzlaff, A. X. Trautwein, K. Wieghardt and P. Chaudhuri, *Inorg. Chem.*, 1998, **37**, 2000.
3 K. P. Wainwright, *Coord. Chem. Rev.*, 1997, **166**, 35.
4 T. A. Kaden, *Top. Curr. Chem.*, 1984, **121**, 154.
5 P. V. Bernhardt and G. A. Lawrence, *Coord. Chem. Rev.*, 1990, **104**, 297.
6 M. Takahasi and S. Takamoto, *Bull. Chem. Soc. Jpn.*, 1977, **50** 3413.
7 K. Wieghardt, U. Bossek, P. Chaudhuri, W. Herrmann, B. C. Menke and J. Weiss, *Inorg. Chem.*, 1982, **21**, 4308.
8 B. A. Sayer, J. P. Michael and R. D. Hancock, *Inorg. Chim. Acta*, 1983, **77**, L63.
9 D. A. Moore, P. E. Fanwick and M. J. Welch, *Inorg. Chem.*, 1989, **28**, 1504.
10 T. Beissel, K. S. Bürger, G. Voigt, K. Wieghardt, C. Butzlaff and A. X. Trautwein, *Inorg. Chem.*, 1993, **32**, 124.
11 O. Schlager, K. Wieghardt, H. Grondey, A. Rufinska and B. Nuber, *Inorg. Chem.*, 1995, **34**, 6440.
12 L. R. Gahan, G. A. Lawrence and A. M. Sargeson, *Aust. J. Chem.*, 1982, **35**, 1119.
13 L. Christiansen, D. N. Hendrickson, H. Toflund, S. R. Wilson and C. L. Xie, *Inorg. Chem.*, 1986, **25**, 2813.
14 K. Wieghardt, E. Schöffmann, B. Nuber and J. Weiss, *Inorg. Chem.*, 1986, **25**, 4877.
15 R. Ziessel and J.-M. Lehn, *Helv. Chim. Acta*, 1990, **73**, 1149.
16 M. Di Vaira, F. Manni and P. Stoppioni, J. Chem. Soc., *Chem. Commun.*, 1989, 126.
17 M. Di Vaira, B. Cosimelli, F. Manni and P. Stoppioni, *J. Chem. Soc., Dalton Trans.*, 1991, 331.
18 A. A. Watson, A. C. Willis and D. P. Fairlie, *Inorg. Chem.*, 1997, **36**, 752.
19 P. Chaudhuri and M. Winter, unpublished work; F. Birkelbach, Dissertation, Bochum, 1995.
20 H. Sigel and R. B. Martin, *Chem. Rev.*, 1982, **82**, 385.
21 J. K. Moran and C. F. Meares, in *Encyclopedia of Inorganic Chemistry*, ed. R. B. King, Wiley, New York, 1994, vol. 6, p. 3067.
22 (*a*) S. Amin, C. Marks, L. M. Toomey, M. R. Churchill and J. R. Morrow, *Inorg. Chim. Acta*, 1996, **246**, 99; (*b*) L. M. Berreau, J. A. Halfen, V. G. Young and W. B. Tolman, *Inorg. Chem.*, 1998, **37**, 1091.
23 K. Wieghardt, W. Schmidt, B. Nuber and J. Weiss, *Chem. Ber.*, 1979, **112**, 2220.
24 T. J. Atkins, J. E. Richman and W. F. Oettle, *Org. Synth.*, 1978, **58**, 86.
25 W. E. Weaver and W. M. Whaley, *J. Am. Chem. Soc.*, 1947, **69**, 515.
26 R. Kataky, K. E. Matthes, P. E. Nicholson, D. Parker and H.-J. Buschmann, *J. Chem. Soc., Perkin Trans. 2*, 1990, 1425.
27 G. M. Sheldrick, SADBAS, University of Göttingen, 1994.
28 G. M. Sheldrick, SHELXTL PLUS, Siemens Analytical Instruments, Madison, WI, 1990.
29 (*a*) *International Tables for X-Ray Crystallography*, Kynoch Press, Birmingham, 1974, vol. 4; (*b*) H. D. Flack, *Acta Crystallogr., Sect. A*, 1983, **39**, 876.
30 C. J. Ballhausen and H. B. Gray, *Inorg. Chem.*, 1962, **1**, 111.
31 A. B. P. Lever, *Inorganic Electronic Spectroscopy*, Elsevier, Amsterdam, 1984.
32 C. K. Johnson, ORTEP, Report ORNL-5138, Oak Ridge National Laboratory, Oak Ridge, TN, 1976.
33 M. G. B. Drew, *Prog. Inorg. Chem.*, 1977, **23**, 67 and refs. therein.
34 R. A. Levenson and R. L. R. Townsend, *Inorg. Chem.*, 1974, **13**, 105.
35 M. Shimoi, Y. Saito and H. Ogino, *Bull. Chem. Soc. Jpn.*, 1991, **64**, 2629.
36 A. Neves, W. Walz, K. Wieghardt, B. Nuber and J. Weiss, *Inorg. Chem.*, 1988, **27**, 2484 and refs. therein; J. C. Dutton, G. D. Fallon and K. S. Murray, *Inorg. Chem.*, 1988, **27**, 34; A. D. Keramidas, A. B., Papaiaanou, A. Vlahos, T. A. Kabanos, G. Bonas,

A. Makriyannis, C. P. Rapropoulou and A. Terzis, *Inorg. Chem.*, 1996, **35**, 357 and refs. therein.
37 T. J. Collins, B. D. Santarsiero and G. H. Spies, *J. Chem. Soc.*, *Chem. Commun.*, 1983, 681.
38 C. M. Murdoch, M. K. Cooper, T. W. Hambley, W. N. Hunter and H. C. Freeman, *J. Chem. Soc.*, *Chem. Commun.*, 1986, 1329.
39 H. C. Freeman, *Adv. Protein Chem.*, 1967, **22**, 257.
40 O. Schlager, K. Wieghardt and B. Nuber, *Inorg. Chem.*, 1995, **34**, 6449.
41 M. J. van der Merwe, J. C. A. Boeyens and R. D. Hancock, *Inorg. Chem.*, 1985, **24**, 1208.
42 J. N. McElearney, R. W. Schwartz, A. E. Sieigel and R. L. Carlin, *J. Am. Chem. Soc.*, 1971, **93**, 4337; R. L. Carlin, C. J. O'Connor and S. N. Bhatia, *Inorg. Chem.*, 1976, **15**, 985; A. K. Gregson, D. M. Doddrell and P. C. Healy, *Inorg. Chem.*, 1978, **17**, 1216.
43 J. N. McElearney, R. W. Schwartz, S. Merchant and R. L. Carlin, *J. Chem. Phys.*, 1971, **55**, 466.
44 H. U. Rahman, *J. Phys. C.*, 1971, **4**, 3301.
45 *Theory and Applications of Molecular Paramagnetism*, eds. E. A. Boudreaux and L. N. Mulay, Wiley, New York, 1976.
46 *Electron Paramagnetic Resonance of d Transition Metal Compounds*, eds. F. E. Mabbs and D. Collison, Elsevier, Amsterdam, 1992.

Paper 8/06466K